Mode Conversion Estimation of Filleted T-Joint Using FEM and 3D Laser Vibrometry

J. AYERS, E. SWENSON, M. RUZZENE and A. GHOSHAL

ABSTRACT

T-joint configurations, commonly found in aerospace applications, provide a challenge for structural health monitoring (SHM) strategies that employ wave propagation based interrogation techniques. The challenge arises from the complexity of wave propagation through the T-joint interface, and the consequent mode conversion and reflections. This work presents a numerical characterization of undamaged T-joint using simplified two-dimensional (2D) plane strain finite element (FE) models, where excitation from a piezoelectric actuator is simulated on one side of the T-joint. The incident and consequent reflected waveforms are separated in the frequency-wavenumber domain, and spatially-integrated multiple component mode coefficients are formulated in the frequency-spatial domain with the intent to characterize wave reflections and mode conversions. Mode coefficients from the undamaged configuration are compared to T-joints with blind side notch damage located in the fillet radius. Trends from the 2D FE numerical studies are verified by a three dimensional (3D) Scanning Laser Vibrometer test setup for the undamaged case, which consists of an aluminum T-joint for selected fillet radius (0.6 cm) and stiffener thickness (0.3 cm). The setup enables 3D full wavefield surface measurements of the front and back sides of the plate, plate-stiffener radius, and stiffener. Recommendations of how to use the mode coefficient formulation as a damage quantification tool for the T-joint are given.

INTRODUCTION

The stiffener-plate configuration, or so-called T-joint, is ubiquitous in aerospace

James Ayers , US Army Research Laboratory, Aberdeen, MD, james.t.ayers@us.army.mil
Eric Swenson, AFIT/ENY, WPAFB, OH, Eric.Swenson@afit.edu
Massimo Ruzzene, Georgia Institute of Technology, Atlanta, GA, ruzzene@gatech.edu
Anindya Ghoshal, US Army Research Lab, Aberdeen, MD, anindya.ghoshal@us.army.mil

Report Documentation Page

Form Approved
OMB No. 0704-0188

1. REPORT DATE	2. REPORT TYPE	3. DATES COVERED
SEP 2011	**N/A**	**-**

4. TITLE AND SUBTITLE
Mode Conversion Estimation of Filleted T-Joint Using FEM and 3D Laser Vibrometry

5a. CONTRACT NUMBER
5b. GRANT NUMBER
5c. PROGRAM ELEMENT NUMBER

6. AUTHOR(S)

5d. PROJECT NUMBER
5e. TASK NUMBER
5f. WORK UNIT NUMBER

7. PERFORMING ORGANIZATION NAME(S) AND ADDRESS(ES)
US Army Research Laboratory, Aberdeen, MD

8. PERFORMING ORGANIZATION REPORT NUMBER

9. SPONSORING/MONITORING AGENCY NAME(S) AND ADDRESS(ES)

10. SPONSOR/MONITOR'S ACRONYM(S)
11. SPONSOR/MONITOR'S REPORT NUMBER(S)

12. DISTRIBUTION/AVAILABILITY STATEMENT
Approved for public release, distribution unlimited

13. SUPPLEMENTARY NOTES
See also ADA580921. International Workshop on Structural Health Monitoring: From Condition-based Maintenance to Autonomous Structures. Held in Stanford, California on September 13-15, 2011 . U.S. Government or Federal Purpose Rights License.

14. ABSTRACT
T-joint configurations, commonly found in aerospace applications, provide a challenge for structural health monitoring (SHM) strategies that employ wave propagation based interrogation techniques. The challenge arises from the complexity of wave propagation through the T-joint interface, and the consequent mode conversion and reflections. This work presents a numerical characterization of undamaged T-joint using simplified two-dimensional (2D) plane strain finite element (FE) models, where excitation from a piezoelectric actuator is simulated on one side of the T-joint. The incident and consequent reflected waveforms are separated in the frequency-wavenumber domain, and spatially-integrated multiple component mode coefficients are formulated in the frequency-spatial domain with the intent to characterize wave reflections and mode conversions. Mode coefficients from the undamaged configuration are compared to T-joints with blind side notch damage located in the fillet radius. Trends from the 2D FE numerical studies are verified by a three dimensional (3D) Scanning Laser Vibrometer test setup for the undamaged case, which consists of an aluminum T-joint for selected fillet radius (0.6 cm) and stiffener thickness (0.3 cm). The setup enables 3D full wavefield surface measurements of the front and back sides of the plate, plate-stiffener radius, and stiffener. Recommendations of how to use the mode coefficient formulation as a damage quantification tool for the T-joint are given.

15. SUBJECT TERMS

16. SECURITY CLASSIFICATION OF:			17. LIMITATION OF ABSTRACT	18. NUMBER OF PAGES	19a. NAME OF RESPONSIBLE PERSON
a. REPORT	b. ABSTRACT	c. THIS PAGE			
unclassified	**unclassified**	**unclassified**	**SAR**	**8**	

components, and most commonly represented in the wing airfoil-spar and bulkhead-stiffener interfaces. A nominal fillet is generally designed at the interface to alleviate potential stress concentrations, which can produce initiatory cracks under high cycle loading conditions. However, these T-joint configurations provide a challenge for structural health monitoring (SHM) strategies that employ wave propagation-based interrogation techniques, such that partial transmission, reflection, and mode conversion are modified by the degree of the fillet radius, excitation frequency, material constituency, and stiffener cross-sectional thickness[4]. Since the success of this proposed SHM strategy to assess damage severity largely depends on the quantification of the mode conversion, a fundamental understanding of the wave interaction due to the T-joint presence is necessary.

Previous work has been conducted on understanding T-joint configurations of various material constituencies and a range of damage quantification techniques. Modal techniques employed by Ooijevaar et al. [1] and Ghoshal et al. [2] used scanning laser vibrometry to detect damage produced in composite plate with two T–shaped stiffener sections and induced long saw cuts on an aluminum wing panel, respectively. In terms of wave propagation techniques, Greve et al. [3] analyzed Lamb wave interactions of a cracked welded joint, and rolled and plate girders using 2D and 3D FEM. Simulations and experiments showed cracks that are oriented perpendicular to the direction of wave propagation, cause strong reflections. Oppenheim et al. [4] modeled a 2D simulation of Lamb wave transmission/reflection at a T joint with no fillet radius using Abaqus and 3D model of plate girder. Experimental measurements using PZT sensors located on the web in pulse-echo mode, and strong S_0 mode reflections. Similarly, Morvan et al. [5] measured Lamb waves by a laser vibrometer in a T-joint generated by a contact piezo-composite transducer, and normal component of the surface wave displacement of the plate and stiffener. Sohn et al. [6] analyzed mode conversion of T-joint with collocated PZT before and after the stiffener using a 2D simulation under plane strain assumptions. Other studies concluded, with experimental evidence, that damage-sensitive features are successfully extracted as damage-induced Lamb wave modes have unique characteristics compared to those modes produced by the stiffener or varying thickness [7, 8].

The objective of this paper is to further understand the mode conversion mechanism at the T-joint interface using frequency-wavenumber filtering techniques per Ruzzene [9], both as a function of the fillet radius, with and without blind side damage, and with experimental validation that provides high fidelity spatial resolution using 3D laser vibrometry.

MODE COEFFICIENT FORMULATION

This analysis is restricted to the frequency range of the fundamental symmetric and antisymmetric Lamb waves, S_0 and A_0, respectively. As illustrated in Figure 1, it is assumed that a pure S_0 or A_0 mode is generated to interrogate the structure. The interaction of an incident S_0 mode with a stiffener located causes a partial S_0 reflection and partial mode conversion into the A_0 mode, while simultaneously producing a partial S_0 and A_0 mode transmission into the stiffener and the plate. As previously described by Ayers et al. [10], upon filtering the data in the frequency-

wavenumber domain and windowing the data in the time-space domain, $\tilde{W}(x, \omega)$ is the filtered response in the spatial-frequency domain of a single extracted mode at frequency ω.

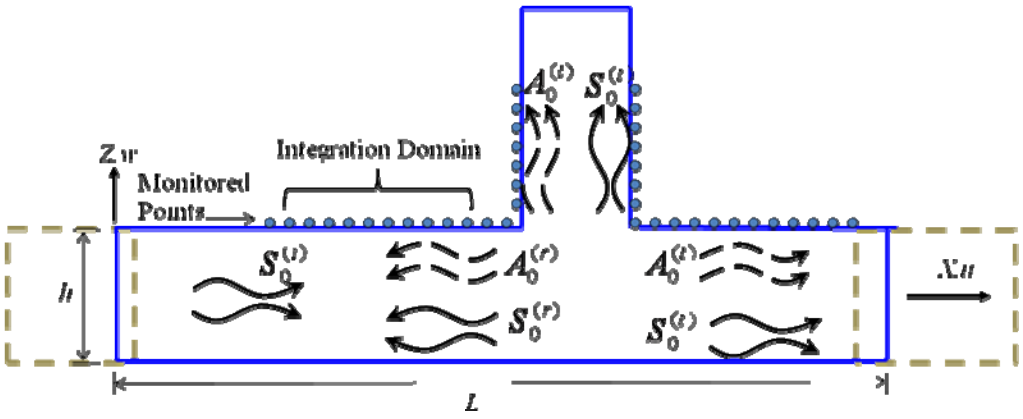

Figure 1. Schematic of T-joint and mode conversion identification

Laser vibrometry techniques allow for various points to be scanned over the distance, *L*. From the measured responses, the value of the mode coefficients may be estimated over a spatial domain. This allows the estimation of its spatial-independence, and more importantly of a spatially averaged value, which is less affected by amplitude fluctuations due to noise, or by general trends associated with geometrical spreading. In compact matrix notation, the mode coefficients may be expressed by the following for an interrogating S_0 mode, but is likewise easily applied for an interrogating A_0 mode:

$$\Pi_{ij}(w) = \frac{\int_{\Omega_{1j}}^{\Omega_{2j}} |\psi_{ij}(x,\omega)| dx}{\int_{x_1}^{x_2} |\Phi_i(x,\omega)| dx} \tag{1}$$

where,

$$\Pi_{ij}(w) = \begin{bmatrix} R^u_{S_0} & T^u_{S_0} & C^u_{A_0} \\ R^w_{S_0} & T^w_{S_0} & C^w_{A_0} \\ R^{uw}_{S_0} & T^{uw}_{S_0} & C^{uw}_{S_0} \end{bmatrix} \tag{2}$$

$$\Psi_{ij}(w) = \begin{bmatrix} \tilde{u}^{(r)}_{S_0} & \tilde{u}^{(t)}_{S_0} & \tilde{u}^{(r)}_{A_0} \\ \tilde{w}^{(r)}_{S_0} & \tilde{w}^{(t)}_{S_0} & \tilde{w}^{(r)}_{A_0} \\ \sqrt{(\tilde{u}^{(r)}_{S_0})^2 + (\tilde{w}^{(r)}_{S_0})^2} & \sqrt{(\tilde{u}^{(t)}_{S_0})^2 + (\tilde{w}^{(t)}_{S_0})^2} & \sqrt{(\tilde{u}^{(r)}_{A_0})^2 + (\tilde{w}^{(r)}_{A_0})^2} \end{bmatrix} \tag{3}$$

and,

$$\Phi_i(w) = \left[\tilde{u}^{(i)}_{S_0} \quad \tilde{w}^{(i)}_{S_0} \quad \sqrt{(\tilde{u}^{(i)}_{S_0})^2 + (\tilde{w}^{(i)}_{S_0})^2} \right] \tag{4}$$

$$\Omega_{ij}(x) = \begin{bmatrix} x_1 & x_3 & x_1 \\ x_2 & x_4 & x_2 \end{bmatrix} \tag{5}$$

where R, T, and C parameters represent the reflection, transmission, and converted coefficients, u and w are the in-plane and out-of-plane displacement components, respectively, and x_i are the integration spatial coordinates. It is important to note that this spatial integration method departs from existing literature, where the mode amplitudes are taken at a fixed location [11].

APPLICATION TO SIMULATED DATA

The mode coefficient formulation is applied to numerical parameterization for the undamaged and damaged configurations using simplified 2D plane strain, where mode conversion estimation is shown as a function of the fillet radius, excitation frequency, and stiffener cross-sectional thickness (Table I and Figure 2).

Table I. Test Matrix of 2D FEM Parameterization

Set	**Signal**	**Plate-Stiffener Geometry**		**Notch Damage Geometry**	
	Frequency	Fillet Radius	Stiffener Thickness	Depth	Orientation
	[kHz]	[mm]	[mm]	[mm]	[deg]
1	200.0	[0.0:3.0:12.0]	3.0	-	-
2	200.0	[0.0:3.0:12.0]	3.0	3.0	0.0
3	200.0	6.0	3.0	[0.0:2.0:8.0]	0.0
4	200.0	6.0	3.0	3.0	[0.0:15.0:75.0]

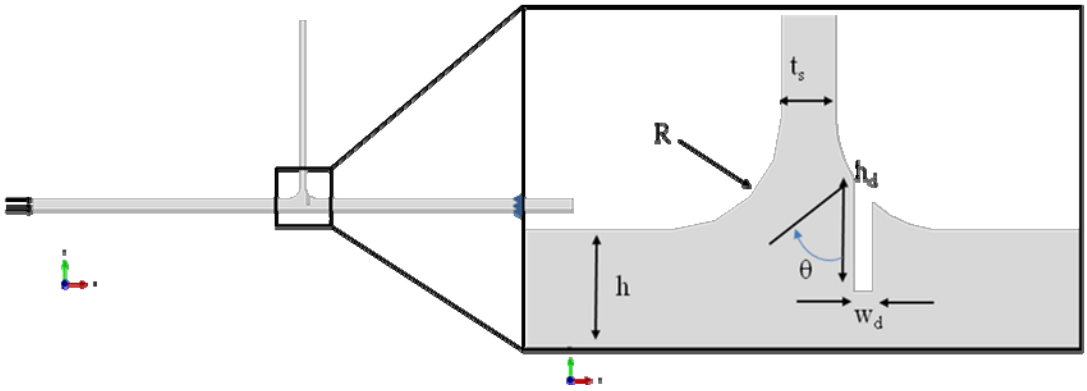

a) (b)

Figure 2: Schematic of 2D FEM T-joint: (a) Profile with identified boundary conditions, (b) Magnified view of FEM parameters at fillet with notch damage

From Figures 3(a-b), the mode coefficients from a no-damage configuration vary parabolically as a function of the fillet radius. With a constant damage depth in Figure 4(a), the R_{S_0} mode coefficients varies linearly as a function of the fillet radius. As the fillet radius increases (greater than 6 mm), the mode coefficients from undamaged to damaged are approximately equivalent (Figures 4(b)). The thickness of the fillet radius (greater than 6 mm) requires that the damage depth does not penetrate the plate thickness, and sensitivity is negligible. The R_{S_0} mode

coefficient is sensitive to the increasing damage depth, whereas the C_{Ao} mode coefficient shows perturbation (greater than 4 mm) once the damage depth penetrates the plate thickness (Figures 5(a-b)). The R_{So} and C_{Ao} mode coefficients demonstrate a sinusoidal profile with the notch orientation (Figures 6(a-b)).

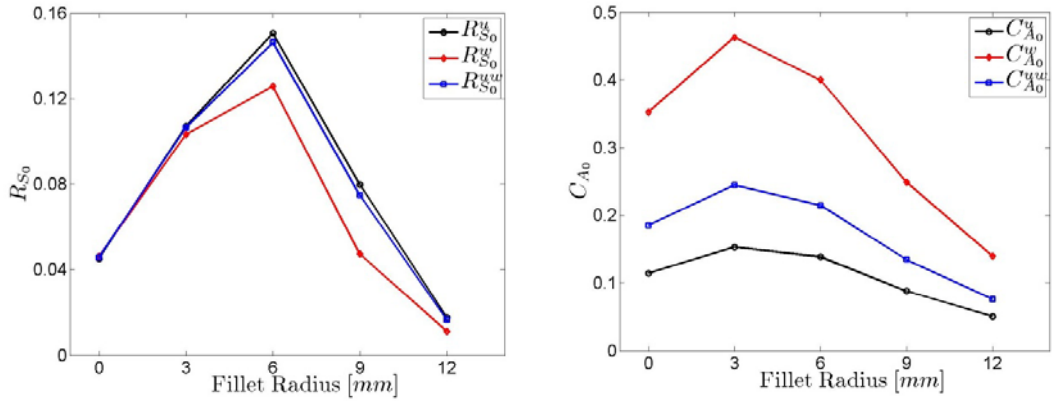

(a) (b)

Figure 3: Variation of fillet radius without blind damage: (a) R_{So} Mode Coefficient (b) C_{Ao} Mode Coefficient

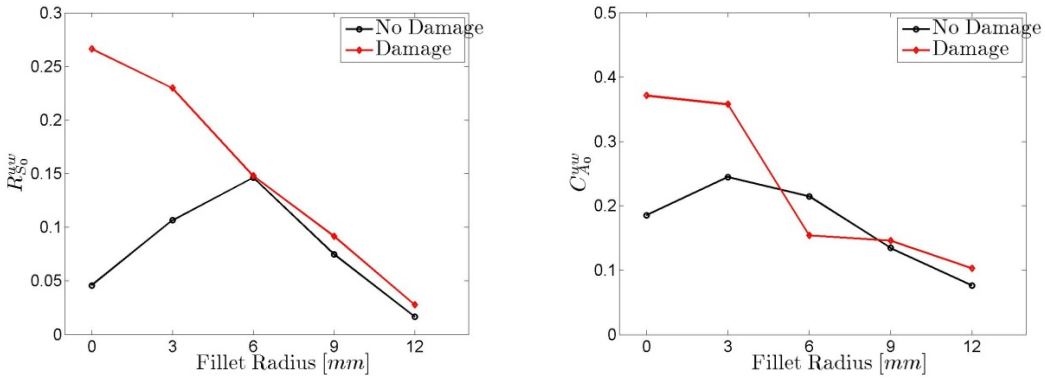

(a) (b)

Figure 4: Variation of fillet radius with blind damage of constant depth and orientation: (a) R_{So} Mode Coefficient (b) C_{Ao} Mode Coefficient

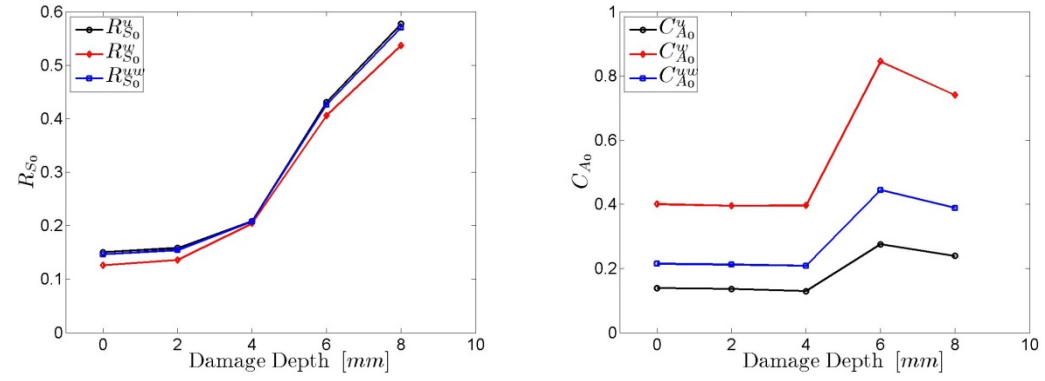

(a) (b)

Figure 5: Variation of blind damage depth with constant fillet radius: (a) R_{So} Mode Coefficient (b) C_{Ao} Mode Coefficient

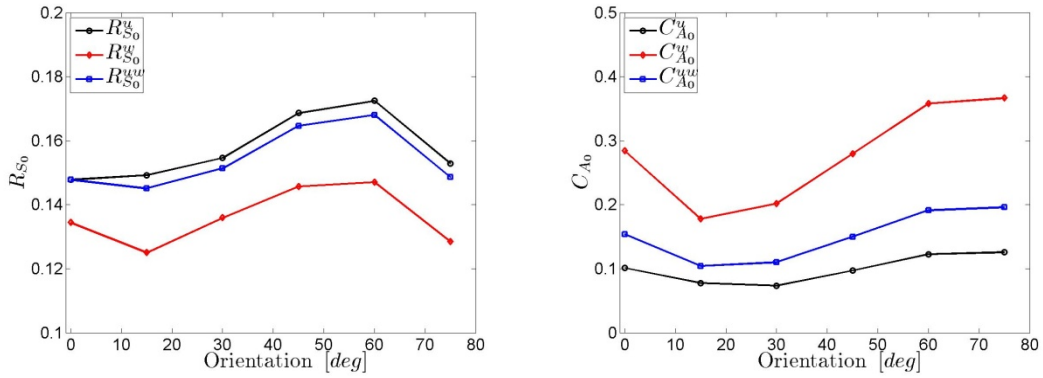

(a) (b)

Figure 6: Variation of blind damage orientation with constant fillet radius: (a) R_{S_0} Mode Coefficient (b) C_{A_0} Mode Coefficient

EXPERIMENTAL RESULTS

The trends from the FE parameterization are investigated by using a 3D Scanning Laser Vibrometry test setup (Figure 7(a)), which consists of an aluminum T-joint for selected fillet radius (0.6 cm), excitation frequency (100 kHz) and stiffener thickness (0.3 cm). The setup enables 3D surface measurement of the front and back sides of the plate, plate-stiffener radius, and stiffener (Figure (b)).

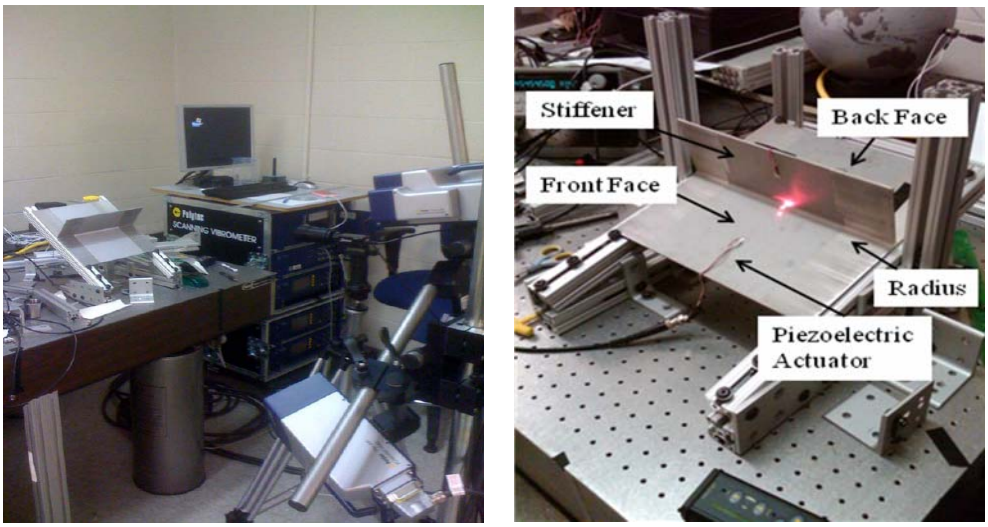

(a) (b)

Figure 7: Experimental validation using Polytec 3D Vibrometer: (a) Test setup (b) Aluminum T-joint specimen

To ensure Lamb wave phenomena, Figure 8(a) illustrates the frequency peaks of the incident A_0 mode of the front face, which aligns with the analytical A_0 mode, while Figure 8(b) shows the back face frequency content, where mode conversion occurs and the S_0 mode is introduced. Figure 9(a) demonstrates the full wavefield of the filtered out-of-plane A_0 mode along the front face, and Figure 9(b) depicts the in-

plane converted S_0 mode. The magnitude of the fillet radius in Figure 9(b) is 3 orders below that of the front and stiffener surfaces. Using data whose spatial points originate at Y-axis 0.14 m in Figure 9(a) and runs along the front, back and stiffener faces, Table II contains the reflection, transmission, and conversion coefficients. Particular attention is given to the difference in order of magnitude between the stiffener and front and back faces, indicating that a significant amount of energy is propagating into the stiffener. The relative order of magnitude, approximately 0.02 to 0.06 along the front face for the reflection and conversion mode coefficients corroborate with the results from the undamaged FE trade studies shown in Figure 3.

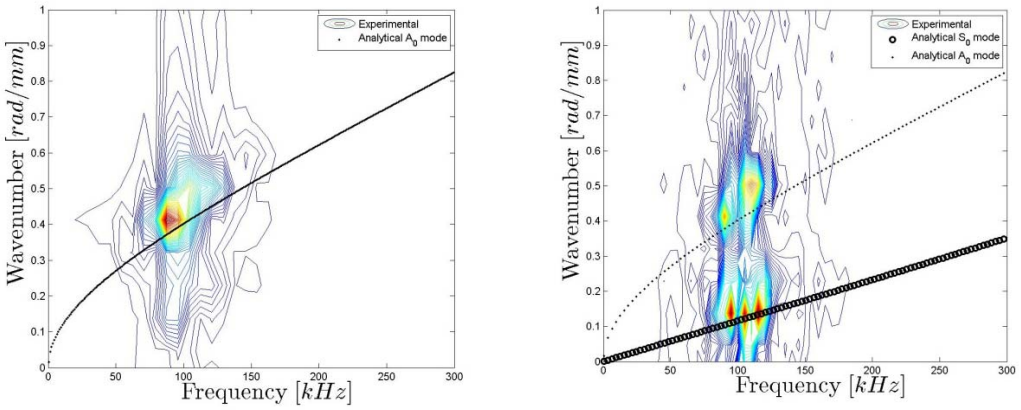

(a) (b)

Figure 8. Incident in-plane frequency content: (a) Front face, and (b) Back face. Excitation frequency of modulated tone burst is 100 kHz.

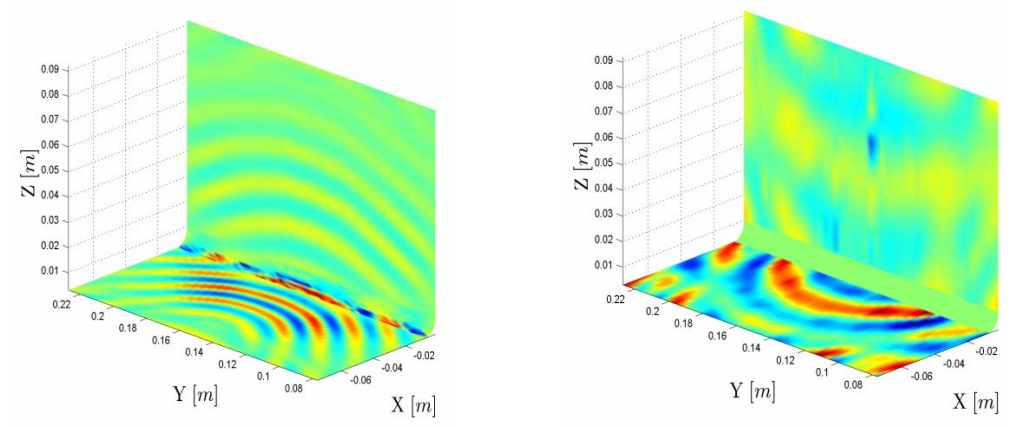

(a) (b)

Figure 9. Time history snapshot at 87.8 μsec along front face-stiffener surfaces: (a) Filtered incident out-of-plane A_0 mode, (b) Filtered converted in-plane S_0 mode

Table II. Integrated mode coefficients along center line of three surfaces

Section	Reflection Coefficients			Transmission Coefficients			Conversion Coefficients		
	R_{A0}^{u}	R_{A0}^{w}	R_{A0}^{uw}	T_{A0}^{u}	T_{A0}^{w}	T_{A0}^{uw}	C_{S0}^{u}	C_{S0}^{w}	C_{S0}^{uw}
Front Face	0.054	0.059	0.058	-	-	-	0.053	0.024	0.039
Back Face	-	-	-	0.012	0.019	0.017	0.014	0.002	0.009
Stiffener	-	-	-	0.193	0.203	0.199	0.118	0.019	0.074

CONCLUSIONS

As the fillet radius increases, the mode coefficients from undamaged to damaged are approximately equivalent. The thickness of the fillet radius (greater than 6 mm) does not allow the damage depth to penetrate the plate thickness, and sensitivity to the relative damage is therefore negligible. In addition, the R_{S0} and C_{A0} mode coefficients demonstrate a sinusoidal profile with the notch orientation, such that the determining the orientation based on the magnitude of the mode coeffiicient is limited. Experimentally, the 3D Laser vibrometry results indicate that the transmission coefficients are an order of magnitude greater within the stiffener section than the front and back faces. Further work is ongoing in varying the damage to the aluminum T-joint, and results will be presented in future papers.

REFERENCES

1. Ooijevaar T. H., Warnet,L.L., Loendersloot, R., Akkerman, R., and de Boer, A. 2010. Vibration based Structural Health Monitoring of a Composite Plate Structure with Multiple Stiffeners, Fifth European Workshop on Structural Health Monitoring, Sorrento, Naples, Italy.
2. Sundaresan, M.J., Pai, P.F., Ghoshal, A., Schulz, M., Ferguson, F. and Chung, J.F. 2001. Methods of distributed sensing for health monitoring of composite material structures, *Composites: Part A*, 32: 1357-1374.
3. Greve, D.W., Tyson, N., and Oppenheim, I.J. 2005. Interaction of defects with Lamb waves in complex geometries, 2005 IEEE Ultrasonics Symposium, 297-300.
4. Oppenheim, J., Greve, D.W., and Tyson, N.L. 2006. Lamb Wave Behavior in Bridge Girder Geometries, Proceedings of SPIE, the International Society for Optical Engineering, Smart structures and materials, San Diego, CA.
5. Morvan, B., Tine, A., and Duclos, J. 1999. Coupling of Lamb waves at a tee junction. IEEE Ultrasonics Symposium, 1: 565 - 568.
6. Kim, S., Lee, C., Hong, J., Park, H., Sohn, H. 2010. Applications of an Instantaneous Damage Detection Technique to Plates with Additional Complexities. *J. Nondestructive Evaluation*, 29: 189–205.
7. Lanza di Scalea, F., Matt, H., Bartoli, I., Coccia, S., Park, S., and Farrar, C. 2007. Health Monitoring of UAV Wing Skin-to-spar Joints using Guided Waves and Macro Fiber Composite Transducers, *J. of Intellignet Material Systems and Structures*, 18: 373-388.
8. Kesavan, A. , Deivasigamani, M., John, S., and Herszberg , I. 2006. Damage detection in T-joint composite structures. *Composite Structures*, 75: 313–320
9. Ruzzene, M. 2007. Frequency/wavenumber filtering for improved damage visualization. *Smart Materials and Structures*, 16:2116-2129.
10. Ayers, J., Apetre, N., and Ruzzene, M. 2011. Phase Gradient and Mode Conversion Estimation in 1D Damaged Structures. *Structural Health Monitoring*, 1: 65–82.
11. Lowe, M., and Diligent, O. 2002. Low-frequency reflection characteristics of the s(0) Lamb wave from a rectangular notch in a plate. *J. of the Acoustical Society of America*, 111:64-74.